



## Temperature anomaly reemergence in seasonally frozen soils

Kevin M. Schaefer,<sup>1</sup> Tingjun Zhang,<sup>1</sup> Pieter P. Tans,<sup>2</sup> and Reto Stöckli<sup>3</sup>

Received 7 March 2007; revised 31 May 2007; accepted 2 August 2007; published 16 October 2007.

[1] In cold regions where soils experience seasonally freezing and thawing, past soil temperature anomalies are stored as variations in the amount of ground ice and can reemerge at the surface after frozen soils thaw. Warmer soils in autumn result in shallower freeze depths in winter, requiring less energy to thaw in spring, and resulting in warmer soils the following summer. We identified reemergence from in situ soil temperature data across the former Soviet Union and simulated reemergence using a soil heat transfer model with phase change. Reemergence is triggered by a sudden drop in the apparent soil specific heat associated with the latent heat of fusion of water. Past soil temperature anomalies persisting just below the maximum freeze depth, which varies from less than one to three meters, amplify the reemergence signal. Reemergence strength increases with soil water content and does not occur if the soil never freezes. To simulate the reemergence, models need a soil column at least 7 m deep with enough vertical resolution to accurately capture variability in the frozen layer. Reemergence of past soil temperature anomalies is a new class of time delayed, land-atmosphere feedbacks that can potentially help to explain observed variability in climate and improve seasonal climate prediction in regions with seasonally frozen soils.

**Citation:** Schaefer, K. M., T. Zhang, P. P. Tans, and R. Stöckli (2007), Temperature anomaly reemergence in seasonally frozen soils, *J. Geophys. Res.*, 112, D20102, doi:10.1029/2007JD008630.

### 1. Introduction and Hypothesis

[2] Soil temperature and moisture depend on surface conditions, such as surface air temperature, precipitation, vegetation, snow depth, and other factors [Osterkamp, 2005; Zhang, 2005]. In particular, snow's high solar reflectivity, high infrared emissivity, low thermal conductivity, and high latent heat content strongly influence seasonal and interannual variations in soil temperature and moisture [Bartlett *et al.*, 2005; Zhang, 2005]. Soil temperature and moisture in turn influence surface energy balance and the partitioning of sensible and latent heat fluxes [Fuchs *et al.*, 1978; Peters-Lidard *et al.*, 1998; Ling and Zhang, 2005]. By modulating surface energy fluxes, soil temperature and moisture anomalies affect atmospheric boundary layer processes [Pan and Mahrt, 1987], regional circulation [Bhatta *et al.*, 2003; Gao *et al.*, 2005], and regional climate [Tang and Reiter, 1986]. Soil temperature and moisture change relatively slowly, influencing surface fluxes for several weeks or months. Land memory is the recording of surface conditions as variations in soil temperature and moisture and the subsequent influence of these conditions on surface

fluxes and atmospheric circulation at a later date [Hu and Feng, 2003].

[3] Several recent studies suggest that the effects of land memory can disappear for several months only to reappear at a later date. For example, warmer than average winter temperatures in East Asia associated with the North Atlantic Oscillation (NAO) correlate with increased vegetation productivity 1.5 years later [Wang and You, 2004]. Increased rainfall in the Indian Monsoon is preceded by lower winter snow cover in Eurasia and higher snow cover in the Tibetan plateau [Robock *et al.*, 2003]. In the southwest United States, increased snow in winter is associated with decreased summer rainfall during the North American monsoon [Lo and Clark, 2002]. These relationships remain largely unexplained, but suggest the existence of an energy storage mechanism that causes the effects of land memory to disappear for a period of time and then reappear at a later date.

[4] Near surface temperature and moisture anomalies do not persist long enough to explain how the effects of land memory can disappear and reappear. Soil temperature and moisture anomalies in the top 1 m of soil exert the strongest influence on surface fluxes and thus dominate the effects of land memory. However, near-surface temperature anomalies persist for only 2–3 months [Hu and Feng, 2004; Schaefer *et al.*, 2005] and moisture anomalies for only 1–2 months [Robock *et al.*, 2003; Amenu *et al.*, 2005]. On the other hand, temperature anomalies can persist, isolated from surface processes, for as long as a year at depths of 3 m [Schaefer *et al.*, 2005], but how these buried soil temperature anomalies could reemerge at the surface to influence surface energy fluxes is unclear.

<sup>1</sup>National Snow and Ice Data Center, Cooperative Institute for Research in Environmental Sciences, University of Colorado at Boulder, Boulder, Colorado, USA.

<sup>2</sup>Earth System Research Laboratory, National Oceanic and Atmospheric Administration, Boulder, Colorado, USA.

<sup>3</sup>Department of Atmospheric Science, Colorado State University, Boulder, Colorado, USA.

[5] Soil temperature varies with time and depth according to the heat diffusion equation [Carslaw and Jaeger, 1959]:

$$\frac{\partial T(t, z)}{\partial t} = -\frac{1}{\rho c_a} \frac{\partial}{\partial z} \left( k \frac{\partial T(t, z)}{\partial z} \right), \quad (1)$$

where  $T$  (K) is soil temperature,  $t$  (s) is time,  $z$  (m) is soil depth,  $\rho$  ( $\text{kg m}^{-3}$ ) is soil bulk density,  $c_a$  ( $\text{J kg}^{-1} \text{K}^{-1}$ ) is apparent soil specific heat, and  $k$  ( $\text{W m}^{-1} \text{K}^{-1}$ ) is soil thermal conductivity.  $k$  determines how fast heat moves through the soil while  $c_a$  determines how much heat is needed to change soil temperature. Assuming a sinusoidal variation in surface temperature, no phase change, and constant soil moisture,  $k$ , and  $c_a$  with depth and time, the heat diffusion equation has an analytical, steady state solution [Carslaw and Jaeger, 1959; Hillel, 1998; Smerdon et al., 2003; Elias et al., 2004]:

$$T(t, z) = T_{ave} + A_0 e^{-z/D} \sin \left[ 2\pi \frac{t}{\tau} - \frac{z}{D} + \phi \right], \quad (2)$$

where  $T_{ave}$  (K) is the average ground surface temperature,  $A_0$  (K) is the amplitude of the surface temperature variation,  $D$  (m) is damping depth,  $\tau$  (s) is the period of oscillation, and  $\phi$  is a phase constant.

[6]  $D$  is an e-folding depth representing the depth to which surface processes with a characteristic  $\tau$  influence soil temperature:

$$D = \sqrt{\frac{\tau k}{\pi \rho c_a}}. \quad (3)$$

Temperature amplitude decreases exponentially with depth from  $\sim 37\%$  of the surface amplitude at  $z = D$  to  $\sim 5\%$  at  $z = 3D$ . Another interpretation is that  $\sim 95\%$  of the energy associated with a periodic surface process is situated above  $3D$ . For seasonal variation,  $\tau$  is 12 months and, using typical values of soil water content,  $k$ , and  $c_a$  (see model description below)  $D$  is  $\sim 2.3$  m for thawed soil. Since  $k$  is greater for ice than liquid water,  $D$  is  $\sim 3$  m for frozen soil. For soils undergoing annual freeze and thaw cycles, the above analytical solution does not apply, but by examining the results from our numerical soil heat transfer model with phase change, we find that  $D$  is 2–3 m.

[7] Land memory falls into the category of inter-annual variability, defined as deviations from an average seasonal cycle. Although not strictly periodic, inter-annual variability represents temperature and moisture anomalies with characteristic  $\tau$  of 1–12 months superimposed upon the seasonal cycle. Consequently,  $D$  for seasonal variation also defines the maximum depths to which inter-annual variations in surface conditions can affect soil temperature. The bulk of the energy associated with inter-annual variability is situated above  $3D$  defined by the seasonal cycle, implying any energy storage mechanism should be within the top 7 to 9 m of soil.

[8] We hypothesize that latent heat associated with the freezing and thawing of groundwater could provide a heat storage mechanism large enough to explain how the effects of land memory can disappear and reappear. In soils undergoing annual freeze-thaw cycles, changes in surface conditions affect both soil temperature and the amount of ground ice. Also, water infiltration followed by freezing and subsequent release of latent heat influences soil temperature [Kane et al., 2001]. The latent heat of fusion is an order of

magnitude greater than the specific heat of either water or ice, so variations in the amount of ground ice can represent a significant amount of energy. We further hypothesize that climate driven perturbations in soil energy are stored as variations in the amount of ground ice. Energy in the form of ground ice is effectively removed from heat diffusion processes, providing a plausible energy storage mechanism to explain the disappearance and reappearance of near surface soil temperature anomalies. When the ground ice melts, buried temperature anomalies reemerge at the surface and the land memory changes from a latent state back to an active component of the climate system. We therefore define temperature reemergence as the disappearance and subsequent reappearance of near surface soil temperature anomalies, driven by soil freeze-thaw processes.

[9] The concept of temperature reemergence is not new: winter Sea Surface Temperature (SST) anomalies in the North Atlantic tend to disappear in summer only to reappear the following winter [Alexander and Deser, 1995; Deser et al., 2003]. At high latitudes in winter, cold air temperatures produce cold, dense surface water that sinks, creating a deep, mixed ocean boundary layer. Vertical mixing stops in spring, but the deep, residual mixed layer persists throughout the summer, isolating the winter SST anomalies from the effects of surface processes. When deep water formation resumes the following winter, entrainment of the residual layer allows the previous winter's SST anomalies to reemerge at the surface [Deser et al., 2003]. Although the physical mechanisms differ, we hypothesize that the frozen soil layer is the land analog of the residual ocean boundary layer and the annual spring thaw is the analog of entrainment such that past soil temperature anomalies can reemerge at the surface.

## 2. Data and Methods

[10] To test our hypothesis, we look for characteristic statistical signs of temperature reemergence in long-term soil temperature data measured across the former Soviet Union [Zhang et al., 2001a, 2001b]. Reemergence in the soil temperature measurements would manifest itself as statistically significant secondary peaks in the autocorrelation function [Deser et al., 2003]. We then simulate reemergence by introducing a single perturbation in surface heat flux into a soil heat transfer model with phase change spun up to a steady state seasonal cycle. Reemergence would manifest itself as secondary peaks in the simulated temperature anomaly. Using the model, we vary the annual average temperature and the amount of soil moisture to determine the required conditions for reemergence to occur. Last, we vary total soil depth and the number of soil layers to determine the model configuration required to simulate reemergence. We focus on the thermodynamics of reemergence and do not assess potential effects on sensible and latent heat fluxes. We limit our analysis to temperature anomalies on seasonal to inter-annual timescales at depths up to 9 m.

## 3. Soil Temperature Measurements

[11] We obtained observed, monthly mean soil temperatures at various depths from 103 standard hydro-meteorological stations scattered across the former Soviet Union (Figure 1)

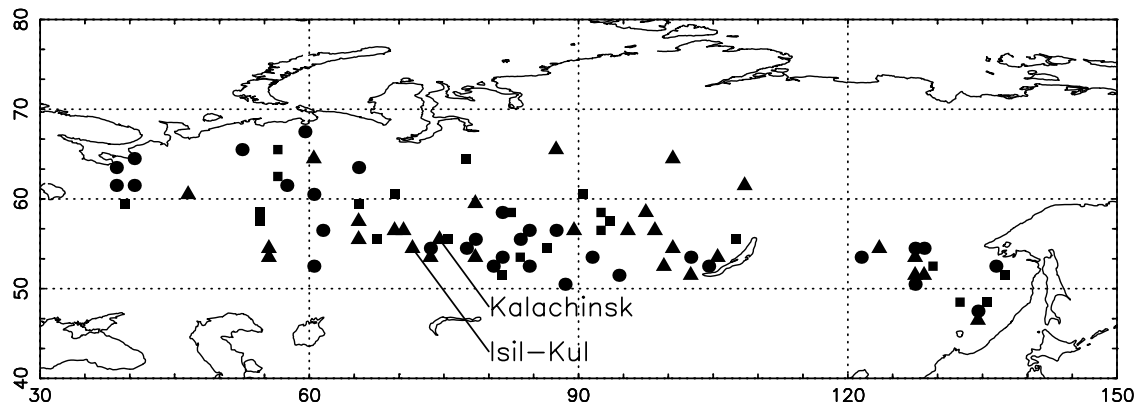


**Figure 1.** Meteorological stations in the former Soviet Union with soil temperature records used in this study. Triangles indicate statistically significant reemergence; squares indicate signs of reemergence, but not statistically significant; circles indicate no reemergence. Kalachinsk and Isil-Kul are analyzed in detail.

[Zhang *et al.*, 2001a, 2001b]. The complete data set with additional documentation is publicly available at the National Snow and Ice Data Center (NSIDC) at <http://nsidc.org/data/arcss078.html>. Soil temperature was measured using bent stem thermometers, extraction thermometers, and electrical resistance thermistors. The data set includes temperatures for 13 soil depths ranging from 2–320 cm, although not all depths were measured at all stations [Gilichinsky *et al.*, 1998; Zhang *et al.*, 2001a]. The measurements span 1898–1990 with the time periods covered by individual stations ranging from 3 to 93 years, although the time periods covered at individual soil depths varied at a single station. Our statistical analysis required fairly long and complete measurements, so we omitted temperature records of less than 25 years, with more than 50% missing data, with a maximum data gap of more than 25 years, or with summer only coverage. After screening, we had time series of monthly mean soil temperatures for 8 soil depths at 94 stations (Table 1).

[12] To identify reemergence in observed soil temperatures, we follow the basic statistical procedures used by Deser *et al.* [2003] to identify SST reemergence. We calculate auto-correlations for each month with lag times ranging from 0 to 36 months. For example, a lag time of 1 month correlates July temperature anomalies with August anomalies; a 2-month lag correlates July and September anomalies, and so forth. Autocorrelations start at one for zero lag and drop off with lag time. Assuming an exponential decrease in autocorrelation with lag time, the characteristic persistence time of soil temperature anomalies is the lag time where the autocorrelation function falls below 0.37 or  $1/e$ . Temperature reemergence would manifest itself as strong, statistically significant secondary peaks in the autocorrelation function at some months lag beyond the characteristic persistence time.

[13] To prepare the measurements for autocorrelation, we (1) removed long-term trends, (2) calculated the mean seasonal cycle, (3) filled missing data, and (4) removed the mean seasonal cycle. Using only valid data points, we calculated and removed long-term, linear trends. Since monthly soil temperature trends differ, we removed trends for each month separately. After detrending and again using

only valid data points, we determined the average seasonal cycle by calculating the average temperatures for each month. We discarded partial years at the beginning and end of each temperature record and filled missing data with the average monthly data. Subtracting the average monthly values produced a time series of monthly soil temperature anomalies from the average seasonal cycle. We estimated statistical significance using a single-tail Student t-test at 95% significance with the degrees of freedom based on the number of years in each temperature record. For each 12 months of lag, the time series lost one year, so we subtracted one degree of freedom.

#### 4. Model Description

[14] We developed a soil heat transfer model with phase change by applying a finite difference method to the heat diffusion equation (Equation 1). Following Bonan [1996], the model's numerical scheme employs semi-implicit finite differences in time with a time splitting fraction of 0.5 and centered finite differences in space. Unless otherwise stated, we used 100 soil layers with the first layer 1 cm deep and each successive layer 1.05 times thicker down to a depth of  $\sim 26$  m. The depth to which surface forcing affects soil temperature increases with  $\tau$ . Progressively thicker soil layers are typically used in atmospheric circulation models because it allows the surface layers to respond to higher frequency forcing while simultaneously minimizing computation time.

**Table 1.** Soil Temperature Records in This Study

Depth, cm	Number Stations
10	3
20	89
40	93
80	94
120	23
160	88
240	16
320	70

[15] We model  $\rho c_a$  as the sum of the latent heat of fusion and heat capacities of the soil minerals, water, and ice [Lukianov and Golovko, 1957; Fuchs et al., 1978]:

$$\rho c_a = \rho_m c_m + \rho_w c_w + \rho_i c_i + (\rho_w + \rho_i) L_f \frac{\partial f_w}{\partial T}, \quad (4)$$

where  $c_m$ ,  $c_w$ , and  $c_i$  are the specific heats of the soil minerals, water, and ice ( $\text{J kg}^{-1} \text{K}^{-1}$ ),  $\rho_m$ ,  $\rho_w$ , and  $\rho_i$  are the bulk densities of soil mineral, water, and ice ( $\text{kg m}^{-3}$ ),  $f_w$  is the fraction of liquid water, and  $L_f$  is the latent heat of fusion of water ( $\text{J kg}^{-1}$ ). We neglect the specific heat of air in soil pore spaces. Because of surface tension between soil water and clay particles, some soil water remains liquid at temperatures below freezing. Depending on soil texture, 90–99% of the soil water is frozen at  $-1^\circ\text{C}$  [Ling and Zhang, 2004]. We assume the soil water is completely frozen at  $-1^\circ\text{C}$  and approximate  $f_w$  with a third degree polynomial:

$$\begin{aligned} f_w &= 1 & T > T_f \\ f_w &= -2\Delta T^3 - 3\Delta T^2 + 1 & T_f - 1 < T < T_f, \\ f_w &= 0 & T < T_f - 1 \end{aligned} \quad (5)$$

where  $\Delta T = T - T_f$  and  $T_f$  is the freezing point of water (273.15 K). We tested several mathematical formulations for  $f_w$  and found this formulation minimized numerical noise caused by abrupt changes in  $\partial f_w / \partial T$  at  $0^\circ\text{C}$  and  $-1^\circ\text{C}$ .

[16] We model  $k$  as the sum of the frozen and thawed portion of soil:

$$k = f_w k_{thaw} + (1 - f_w) k_{froz}, \quad (6)$$

where  $k_{thaw}$  and  $k_{froz}$  are the thermal conductivities of the unfrozen and frozen portions of the soil ( $\text{W m}^{-1} \text{K}^{-1}$ ). For  $k_{thaw}$  and  $k_{froz}$  we used empirical relationships from Bonan [1996]:

$$\begin{aligned} k_{thaw} &= 0.15 + (k_{\min} k_{water}^\theta - 0.15) f_{sat} \\ k_{froz} &= 0.15 + (k_{\min} k_{ice}^\theta - 0.15) f_{sat} \end{aligned}, \quad (7)$$

where  $k_{\min}$ ,  $k_{water}$ ,  $k_{ice}$  are the thermal conductivities of the soil minerals, water, and ice ( $\text{W m}^{-1} \text{K}^{-1}$ ),  $\theta$  is the soil moisture volume fraction,  $f_{sat}$  is the soil moisture volume fraction at saturation, and 0.15 is an empirical constant ( $\text{W m}^{-1} \text{K}^{-1}$ ).

[17] Both  $c_a$  and  $k$  vary with soil texture and moisture using empirical relationships from Bonan [1996]. Soil texture determines how much water soil can hold, and thus strongly influences both  $c_a$  and  $k$ . We assume uniform soil moisture and texture with depth and time. Unless otherwise stated, we assume 30% sand, 30% clay, and 40% silt with constant soil moisture with depth and time at 50% of saturation.

[18] As an upper or surface boundary condition, we assume a sinusoidal seasonal ground surface heat flux,  $G$ , with annual amplitude of  $10 \text{ W m}^{-2}$  and phased such that zero flux coincided with the vernal and autumnal equinoxes.  $G$  is the net energy flux at the soil surface with a positive  $G$  representing a net energy gain by the soil. For simplicity, we

ignored diurnal and synoptic variability. We based the annual  $G$  amplitude on daily averages of observed  $G$  in summer at a midlatitude site in Germany [Liebethal and Foken, 2007]. Assuming a sinusoidal  $G$  assures that all simulations have exactly the same energy input over time. A sinusoidal  $G$  greatly simplifies our model by avoiding calculation of surface energy budgets and associated radiation, latent heat, and sensible heat fluxes, but does not capture the subtle effects of surface conditions on soil temperature, particularly the insulating effects of snow. By specifying  $G$  we cannot use observed weather to simulate soil temperatures at any specific site. Nevertheless, a sinusoidal  $G$  captures the basic seasonal effects of surface conditions: heat loss in winter and gain in summer.

[19] As a lower boundary condition, we assume no energy exchange downward out of the lowest soil layer in the model. This assumption is valid as long as total soil depth is greater than  $3D$  or the vertical energy fluxes at the bottom of the soil column are small compared to those at the surface. This assumption has minimal effect on simulated soil temperatures for the seasonal and interannual timescales considered in this study, but would not be valid for longer timescales of decades to centuries.

[20] Initial conditions were isothermal (constant temperature with depth) at a specified annual average temperature ( $T_{ann}$ ). We spun up the model for 20 years until the simulated soil temperatures achieved a steady state seasonal cycle about  $T_{ann}$ . We defined steady state as the seasonally varying temperature repeating to within  $0.02^\circ\text{C}$  for two consecutive years at all depths. The time step is two hours in all simulations, which allows a stable numerical solution as long as the temperatures do not change too rapidly at the start of spin up. To ensure a relatively slow rate of temperature change, we linearly increase the  $G$  amplitude from zero to  $10 \text{ W m}^{-2}$  during the first two years of spinup.

[21] To simulate a surface temperature anomaly, we introduced a single,  $8 \text{ W m}^{-2}$  perturbation in  $G$  for 21 days starting at various dates during the year. The single  $G$  perturbation technique ensures the simulations are free of noise resulting from natural climate variability, simplifying the isolation of any reemergence signal. Subtracting the steady state seasonal cycle produced temperature anomalies,  $T'$ , representing the model response to a single perturbation in  $G$ . At the surface,  $T'$  peaks just after the  $G$  perturbation and decreases roughly exponentially with a characteristic e-folding time indicative of heat diffusion throughout the soil column. As for autocorrelation of observed soil temperatures, a secondary peak in the simulated  $T'$  some months lag beyond the characteristic e-folding time indicates reemergence.

[22] We used the thickness of the frozen layer and ground ice fraction to estimate the total amount of ground ice. We defined the frozen layer as the depth of the  $0^\circ\text{C}$  isotherm, which we located using linear interpolation. The maximum freeze depth,  $z_{fz}(\text{m})$ , is the annual maximum depth of the frozen layer. The ground ice perturbation,  $\Delta z_{fz}(\text{m})$ , is the difference in maximum freeze depth before and after the  $G$  perturbation. We defined  $E$  as the fraction of anomalous heat associated with the ground ice perturbation:

$$E = \frac{w L_f \Delta z_{fz}}{\int G' dt}, \quad (8)$$

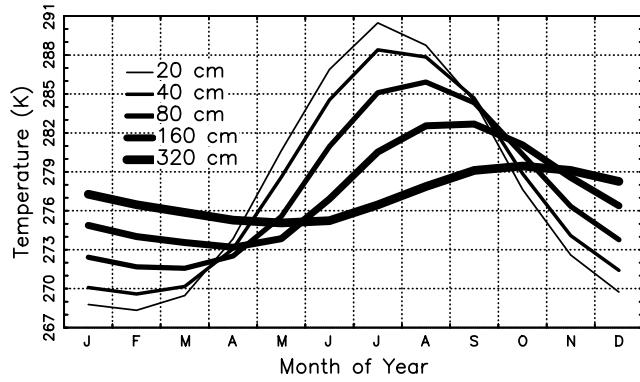


**Figure 2.** The average seasonal cycle in observed soil temperature at Kalachinsk.

where  $w$  is the soil moisture content ( $\text{kg m}^{-3}$ ) and  $G'$  is the ground flux perturbation ( $\text{W m}^{-2}$ ).

[23] We defined simulated reemergence strength,  $S$ , by comparing  $T'$  to a reference case where reemergence does not occur:

$$S = \max\left(\frac{T'}{T'_{ref}}\right) - 1, \quad (9)$$

where  $T'_{ref}$  is the temperature anomaly for a reference case. We calculated  $T'$  and  $T'_{ref}$  at the surface (model layer 1). Since the  $G$  perturbation is the same for all simulations, the choice of a reference temperature,  $T_{annref}$ , is arbitrary as long as the temperatures never drop below freezing. Unless otherwise stated, we chose a  $T_{annref}$  of 300 K such that the soil never froze and heat diffusion dominated the model response to the  $G$  perturbation. Although  $T'$  and  $T'_{ref}$  vary with time and depth,  $S$  is a single number representing the overall strength of reemergence. When  $T' = T'_{ref}$ ,  $T'$  is no greater than what one would expect based on heat diffusion alone and  $S = 0$ . When freezing occurs, some of the anomalous energy changes the amount of ground ice, reemergence occurs, and  $S > 0$ .

[24] In order to evaluate conditions required for reemergence we ran several series of simulations varying  $T_{ann}$  and soil moisture using the 100 layer soil column configuration with a  $G$  perturbation in July. We varied  $T_{ann}$  from 275–290 K with a  $T_{annref}$  of 300 K to reproduce conditions ranging from near permafrost to soil never freezing. To explore the effect of soil water on reemergence, we varied the soil moisture fraction of saturation from zero (no water) to one (completely saturated soil). For simulations near zero soil moisture, the low specific heat of the soil resulted in huge seasonal amplitudes in temperature, so we used a  $T_{annref}$  of 330 K to assure the reference case never froze.

[25] To determine the model configuration required to simulate reemergence, we varied total soil depth and the number of soil layers. Again, we introduced the  $G$  perturbation in July for all simulations. To assess how total soil depth influences simulated reemergence, we started with our original soil column configuration (first layer 1 cm thick, each successive layer 1.05 times thicker) and varied the number of layers from 37–100. Each simulation thus had the same vertical configuration as our baseline simu-

lations, but the total depth varied from 1.01 to 26.1 m. To assess how vertical resolution effects simulated reemergence, we held the total soil depth constant at 4 m (a value typically used in atmospheric circulation models) and varied the number of soil layers from 3–100. When varying the number of soil layers for a constant total depth, we found that assuming a geometric or exponential increase in layer thickness produced vanishingly thin surface layers and led to numerical instability, so we assumed constant layer thickness.

## 5. Results

### 5.1. Observed Reemergence

[26] Of the 94 stations in this study, 33 have statistically significant, secondary peaks in the autocorrelation function indicative of reemergence (Figure 1). Twenty six stations showed annually freezing temperatures with secondary autocorrelation peaks, but they were not statistically significant. We discarded five stations showing sudden, unexplained shifts in the average annual temperature, which produced autocorrelation signatures similar to reemergence. Three stations did not show reemergence because they either did not freeze every year or had highly variable freeze depths. Nearly all of the remaining 27 stations did not show any signs of reemergence because the monthly average temperatures were rounded to the nearest degree centigrade. Rounding monthly averages had the effect of erasing anomalies, resulting in predominantly zero autocorrelations.

[27] Kalachinsk ( $74.6^\circ\text{E}$ ,  $55.0^\circ\text{N}$ ) represents a typical example of statistically significant reemergence. The Kalachinsk temperature record has 15–39 years of measurements (1951–1989) at 8 soil depths (5 of which were suitable for this study). Figure 2 shows the average seasonal cycle in temperatures observed at Kalachinsk. The 20, 40, and 80 cm depths freeze each year while the 320 cm soil layer never freezes. Soil thaw (the date when the entire soil column is thawed) at Kalachinsk typically occurs in May.

[28] Autocorrelations for July temperature anomalies at Kalachinsk show secondary peaks indicating reemergence (Figure 3). The autocorrelations at all layers start at one and decrease with lag time. The characteristic persistence time of temperature anomalies increases with depth from 2 months at 20 cm to 12 months at 320 cm, consistent with previous studies [Hu and Feng, 2004; Schaefer et al., 2005].

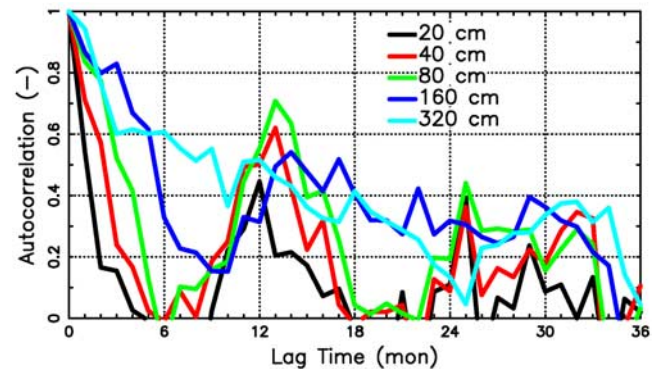


**Figure 3.** Auto-correlations as a function of lag time and depth for June soil temperature anomalies at Kalachinsk.

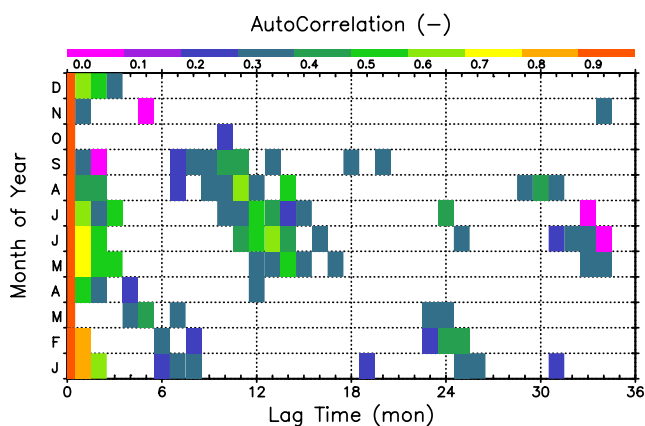


**Figure 4.** Statistically significant autocorrelations at 40 cm depth at Kalachinsk as a function of lag time and month of year.

The 20, 40, and 80 cm depths freeze each year and show secondary autocorrelation peaks at 12 and 24 months indicating temperature reemergence. Kalachinsk has warmed such that the first 15 years of the record showed freezing at 160 cm depth while the last 15 years did not. Consequently, the autocorrelation curve at 160 cm depth appears to indicate both reemergence and persistence. The 320 cm soil layer at Kalachinsk never freezes and shows only persistence with no secondary peaks.

[29] The reemergence of anomalies from different months appear synchronized to occur just after soil thaw. Figure 4 shows statistically significant autocorrelations at Kalachinsk at 40 cm depth as a function of lag time for each month. Autocorrelations for January through September temperature anomalies all show secondary peaks indicating reemergence. The line of secondary peaks is tilted, indicating reemergence is synchronized. For example, the secondary peak for May anomalies occurs at 13 months lag (the following June) and the secondary peak for July anomalies occurs at 11 months lag (also the following June). The line of secondary peaks at Kalachinsk splits in May, when soil thaw typically occurs: anomalies from January reemerge in June while anomalies from May reemerge in June of the following year.

[30] All of the 33 stations in Figure 1 showing statistically significant reemergence have tilted secondary autocorrelation peaks synchronized to just after soil thaw. For each station showing signs of temperature reemergence, the same autocorrelation pattern repeated for all soil layers that froze each winter. Those layers that did not freeze showed only persistence with no secondary autocorrelation peaks.

[31] Soil thaw at most of these 33 stations occurs between May and July, so Kalachinsk represents a fairly typical reemergence pattern. A few stations did show soil thaw as early as March or as late as September. The break in the line of secondary autocorrelation peaks always occurs just after soil thaw, so the line of secondary peaks shifts down for earlier soil thaw and up for later soil thaw. The timing of soil thaw occurs later at higher latitudes, so we expect reemergence to start in the south in early spring and progress northward throughout spring and summer.

[32] The time resolution of monthly average temperature data may be too coarse to adequately resolve the timing of soil thaw at all stations, which may explain why 26 of the stations showed secondary autocorrelation peaks that were not statistically significant. If soil thaw on average occurs at the beginning or end of the month, reemergence would occur in one month in some years and the next month in others. This tends to smear the reemergence signal across a couple of months, making it more difficult to detect statistically. In such cases, reemergence would be easier to detect using weekly or daily average temperatures.

## 5.2. Simulated Reemergence

[33] Our soil heat transfer model with phase change and a seasonally varying sinusoidal  $G$  produces soil temperatures and freeze/thaw cycles consistent with many of the observed temperature records. Figure 5 shows the simulated steady state seasonal cycle in soil temperature at various depths assuming  $T_{ann}$  is 278 K. The simulated soil thaw in May and summer temperatures compare well with the observed seasonal cycle at Kalachinsk, which also has a  $T_{ann}$  of 278 K. Although the simulated temperatures are not cold enough in winter, the simulated depth of the frozen soil layer is  $\sim 0.9$  m, comparable to the observed depth of  $\sim 1.1$  m. Our simple, sinusoidal  $G$  assumption does not fully capture the complex interactions between air temperature, snow cover, soil moisture, and soil temperature, but still produces soil freeze-thaw dynamics representative of many of the stations.

[34] Because the soil moisture and  $G$  profile are the same for all simulations,  $T_{ann}$  determines the amount of ground ice and maximum freeze depth in winter as well as the timing of soil thaw in spring. Figure 6 shows the steady state, simulated maximum freeze depth and date of soil thaw as a function of  $T_{ann}$ , assuming constant soil moisture at 50% of saturation. The colder the  $T_{ann}$ , the deeper the maximum freeze depth, the longer it takes to melt the ground ice, and the later the soil thaw. Soil thaw occurs in July at 275 K and in January at 286 K. Above 287 K the soil never freezes and the freeze depth is zero.

[35] After introducing a  $G$  perturbation and subtracting the steady state seasonal cycle, the simulated temperature anomaly as a function of time also shows secondary peaks indicative of reemergence. Figure 7 shows the simulated

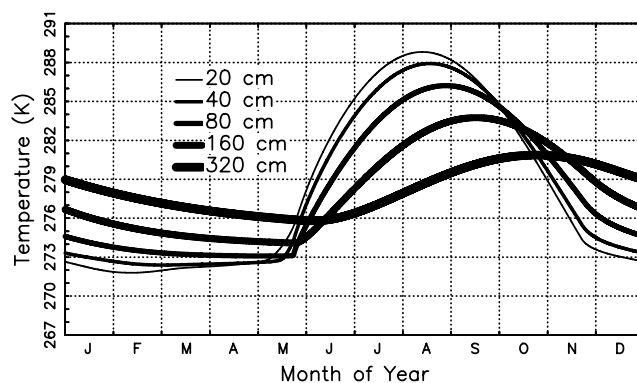


**Figure 5.** Simulated steady state seasonal cycle in soil temperature with an annual average temperature of 278 K and a seasonal ground flux amplitude of  $10 \text{ W m}^{-2}$ .

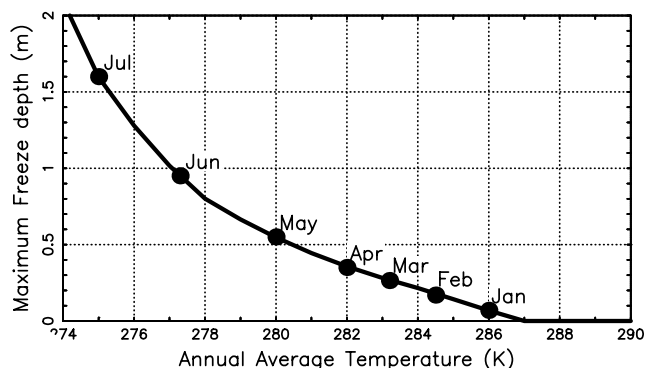


**Figure 6.** Simulated steady state maximum freeze depth and date of soil thaw as a function of annual average temperature.

temperature anomaly at 40 cm depth as a function of time from perturbation assuming a  $T_{ann}$  of 278 K and a July  $G$  perturbation (the model analog to the July autocorrelations in Figure 3). The temperature anomaly peaks right after the  $G$  perturbation and decreases with time as the anomalous heat diffuses through the soil column. In November, four months after the  $G$  perturbation, the soil begins to freeze and the temperature anomaly almost disappears. After the soil column completely thaws the following May (10 months after perturbation), the temperature anomaly reemerges. The upper soil layers freeze each year and all show secondary peaks of similar magnitude indicative of reemergence. Soil layers below the maximum freeze depth show persistence, with minimal signs of reemergence. In the simulation, the model responds to a single  $G$  perturbation, so reemergence occurred every year for  $\sim 20$  years until the entire soil column reached a new steady state with a slightly higher  $T_{ann}$ . In reality, noisy climate forcing eliminates observed reemergence in 1–2 years.

[36] The model simulations indicate that reemergence is synchronized to occur just after soil thaw. Figure 8 shows simulated temperature anomalies at 40 cm depth as a function of time from  $G$  perturbation ( $x$ -axis) and month of perturbation ( $y$ -axis). For clarity, we omitted simulated anomalies below 0.3 K. Figure 8 represents an idealized reemergence response for soil thaw in May, the model analog to the autocorrelations for Kalachinsk in Figure 4. The simulated anomalies show tilted secondary peaks indicating that reemergence is synchronized to the timing of soil thaw. By adjusting  $T_{ann}$ , we changed the timing of simulated soil thaw and were able to reasonably reproduce the characteristic autocorrelation pattern for any of the 33 stations showing statistically significant reemergence (not shown).

[37] To explore the thermodynamics behind reemergence, we must examine temperature anomalies as a function of depth and time. Figure 9 shows observed temperature anomalies for a specific reemergence event over the winter of 1981–2 at Isil-Kul (54.9°N 71.3°E). Isil-Kul has 40–60 years of temperature measurements at seven soil depths, providing enough vertical resolution to visualize reemergence. Figure 10 shows simulated temperature anomalies for an August  $G$  perturbation assuming a  $T_{ann}$  of 278 K and 50% water saturation. In both figures we have removed the

observed and simulated average seasonal cycles as described above. The black lines superimposed upon the temperature anomalies represent the observed and simulated freezing fronts ( $T = 0^\circ\text{C}$ ), which progress downward from the soil surface during fall freeze and spring thaw.

[38] In Figures 9 and 10, the observed and simulated August surface temperature anomaly propagates downward through the soil column over a period of several months. When freezing starts in fall,  $c_a$  includes the latent heat of fusion and is so large that local temperatures stay near freezing, which has the apparent effect of erasing temperature anomalies near the surface. Negative observed temperature anomalies after fall freeze indicate colder than average soil temperatures in winter at Isil-Kul, possibly due to colder air temperatures or shallower snow depths. Both the observations and the model show a small residual of the August surface temperature anomaly persisting through the winter below the frozen layer at depths of 2–3 m. After the soil column completely thaws in May, we see a temperature anomaly “spike” near the maximum freeze depth followed by a rapid return of a positive temperature anomaly to the surface. At the surface, the original August temperature anomaly persists for 1–2 months, disappears, and then reemerges after soil thaw.

[39] The temperature anomaly spike after soil thaw results from a sudden drop in  $c_a$  associated with the latent heat of fusion of water. During spring thaw, heat flows from warmer soils into the frozen layer from both above and below. When the freezing front disappears and the entire soil column is thawed,  $c_a$  no longer includes the latent heat of fusion and suddenly drops by a factor of 10. The  $c_a$  drops instantly, but the heat flow does not, resulting in a rapid, highly localized increase in temperature at the depth where the frozen layer disappears. This sudden drop in  $c_a$  and associated rapid temperature increase occurs every year after soil thaw, so the temperature anomaly spikes in Figures 9 and 10 actually represent a change in the maximum freeze depth and the timing of soil thaw. Variations in the thickness of the frozen layer determine the vertical location of the anomaly spike. The amount of soil water determines the total energy required to melt the ice and, in combination with surface conditions, drives the timing of soil thaw.

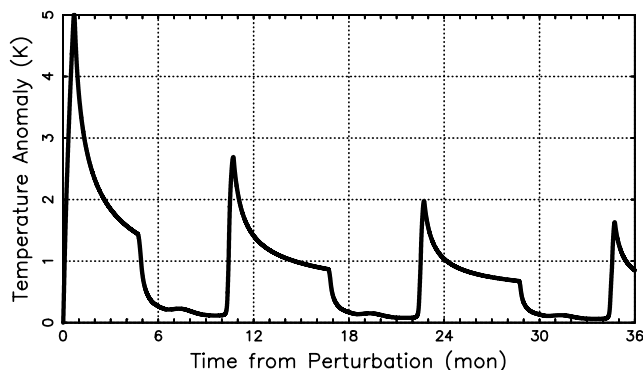


**Figure 7.** Simulated temperature anomaly as a function of time from perturbation at 40 cm depth for a July ground flux perturbation.

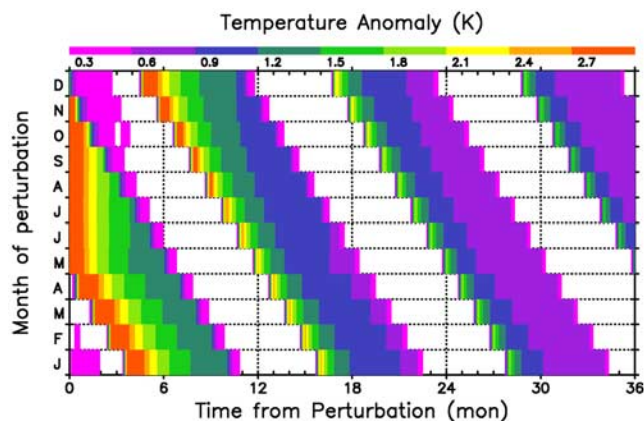


**Figure 8.** Simulated temperature anomalies at 40 cm depth as a function of time from ground flux perturbation and month of perturbation. For clarity, we removed anomalies less than 0.3 K.

[40] The thermodynamics of reemergence is controlled by two factors: the residual temperature anomaly below the frozen layer and variations in the amount of ground ice. At Isil-Kul, colder soil temperatures in winter countered the warmer temperatures in summer, resulting in a maximum freeze depth in the winter of 1981-2 of 1.0 m, slightly less than the average maximum freeze depth of 1.1 m. In the simulation, the  $G$  perturbation reduced the maximum freeze depth from 0.9 to 0.7 m. In the simulation, 60% of the total  $G$  perturbation is stored, isolated from diffusion processes, as a ground ice anomaly. Both the observations and model show a reduced maximum freeze depth, so the frozen layer required less energy to thaw in the spring, resulting in an earlier soil thaw and a positive temperature anomaly in June. Even with average spring and summer surface conditions, a shallower frozen layer in winter means warmer soil temperatures in summer.

[41] The residual temperature anomaly just below the frozen layer modulates the magnitude of the post-thaw temperature anomaly spike. The temperature around the freezing front is always near the freezing point, so any residual temperature anomaly below the frozen layer strongly influences the vertical temperature gradients and the heat

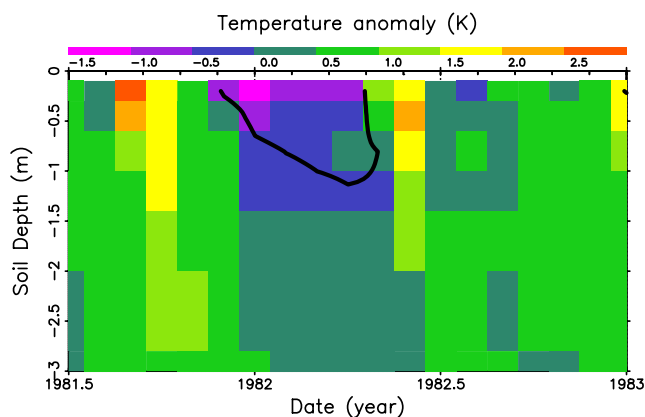


**Figure 9.** Observed temperature anomalies at Isil-Kul for the winter of 1981-2. The black lines represent the freezing front.

flow into the freezing front. A positive residual temperature anomaly means a larger temperature gradient, a stronger heat flow into the freezing front, and a bigger temperature anomaly spike. As one can see from the heat diffusion equation, this modulation is highly non-linear.

[42] The rapid upward and downward propagation of the temperature anomaly after soil thaw results from a perturbation in heat flow triggered by the anomaly spike. A stronger than average temperature spike slows the overall heat flow toward the freezing front, inducing positive temperature anomalies both above and below the spike. These anomalies induce additional anomalies, causing the temperature anomaly to apparently propagate quickly up and down, against the overall flow of heat. This disturbance in heat flow is analogous to when a car on the freeway slows down to avoid an accident, resulting in a backup that propagates very rapidly upstream, against the overall flow of traffic.

### 5.3. Required Conditions for Reemergence

[43] Figure 11 illustrates the calculation of reemergence strength,  $S$ , by comparing simulated temperature anomalies for a case where the soil freezes each year and where the soil never freezes (a  $T_{ann}$  of 278 and 300 K respectively). Both simulations have the same soil thermal properties when the  $G$  perturbation is introduced in July, so both simulations show the same magnitude temperature anomaly, which decreases exponentially with time as heat diffuses through the soil column. However, for a  $T_{ann}$  of 278 K, the anomaly suddenly drops when the soil freezes in winter and sharply increases after the soil column thaws in May. Using the values of  $T'$  and  $T'_{ref}$  indicated by the arrow,  $S \sim 1.5$ .

[44] The effect of  $T_{ann}$  on  $S$  is a balance between two opposing factors: perturbations in the ground ice content and the strength of the residual temperature anomaly below the maximum freeze depth. The perturbation in the ground ice content determines the vertical location and timing of the post-thaw temperature anomaly spike. Residual temperature anomalies below the frozen layer modulate the magnitude of the spike. A large perturbation in ground ice and a strong residual temperature anomaly imply a strong reemergence.

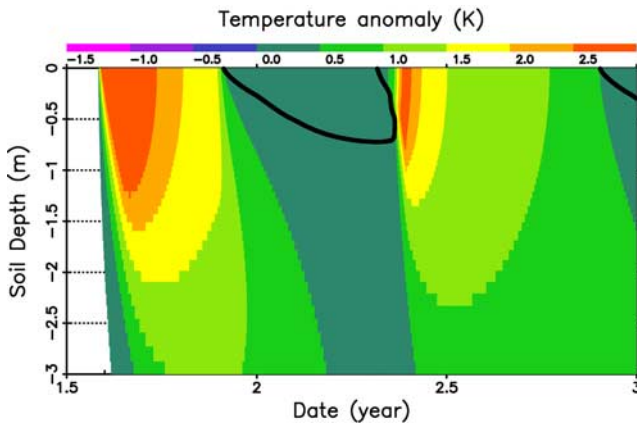


**Figure 10.** Simulated temperature anomalies for an August ground flux perturbation assuming an annual average temperature of 278 K. The black lines represent the freezing front.

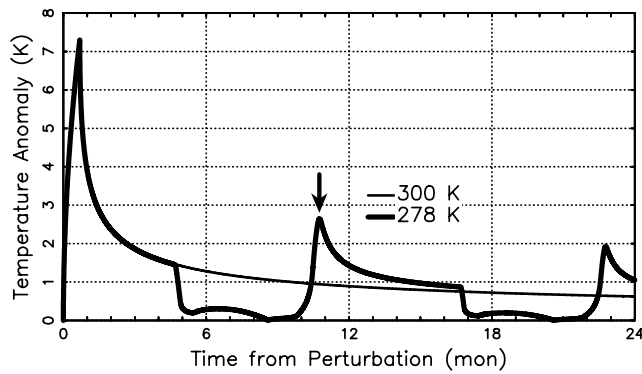


**Figure 11.** Simulated surface temperature anomalies for a July ground flux perturbation in soils that freeze every year (278 K) and soils that never freeze (300 K). The arrow indicates the anomalies used to calculate reemergence strength.

However, these two factors vary in opposite ways: the ground ice perturbation decreases while the residual temperature anomaly increases with  $T_{ann}$ .

[45] An optimal balance between ground ice perturbation and the strength of the residual temperature anomaly produces a maximum  $S$  at a  $T_{ann}$  of 281 K (Figure 12).  $S$  is relatively weak at low and high  $T_{ann}$  due to either a small ground ice perturbation or a small residual temperature anomaly. For a  $T_{ann}$  of 275 K, the bulk of the anomalous heat has diffused down only  $\sim 1$  m before the soil starts freezing in September. Since the steady state freeze depth at 275 K is 1.5 m, nearly all of the  $G$  perturbation is converted into a ground ice perturbation, leaving a small residual temperature anomaly. Although the ground ice perturbation is large,  $S$  is relatively weak because the residual anomaly is weak. For 285 K, the temperature anomaly has diffused deep into the soil column before freezing starts in December. The maximum freeze depth is only 0.25 m and only a small fraction of the  $G$  perturbation is converted into a ground ice perturbation, leaving a strong residual temperature anomaly. Although the residual anomaly is strong,  $S$  is relatively weak because the ground ice perturbation is small.  $S$  is zero above 287 K because the soil never freezes.

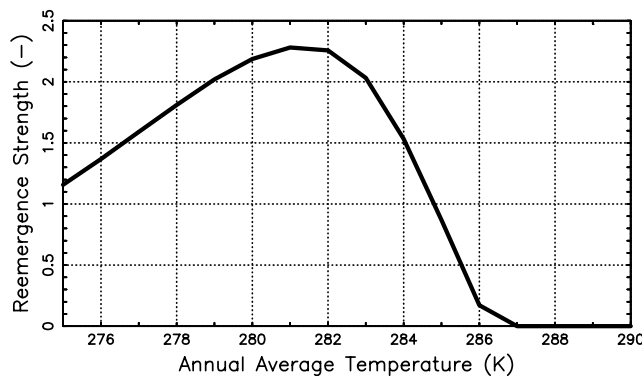


**Figure 12.** Reemergence strength for a July ground flux perturbation as a function of annual average temperature.

[46] The soil in these simulations never freezes below 3 m depth, but can reemergence occur under permafrost conditions where the deep soil layers never thaw? We simulated permafrost by setting  $T_{ann}$  to 270 K and found the sudden drop in  $c_a$  and associated temperature reemergence occurred in winter when the soil column completely froze (not shown). This indicates that for permafrost, temperature variations are stored as variations in the active layer. Permafrost may have a different characteristic reemergence than non-permafrost regions, but the underlying mechanism is the same: temperature variations are stored as variations in latent heat. Unfortunately, the station network used in this analysis did not include any permafrost sites to confirm this simulation result.

[47] Reemergence does not occur without groundwater and  $S$  increases with soil moisture content (Figure 13). When the soil has no water, freezing does not occur and  $S$  is zero.  $S$  increases rapidly with soil moisture as the latent heat associated with annual freezing and thawing increases.  $S$  levels off as soil moisture approaches saturation due to compensating effects of increased thermal conductivity and specific heat. The right end point of the curve represents fully saturated soil, as determined by soil porosity ( $\sim 47\%$  porosity for 30% sand and 30% clay). Simulations with different soil textures produced nearly identical results (not shown). Changing soil texture altered the soil thermal properties slightly, but  $S$  depends primarily on the amount of water in the soil. Soil texture has almost no effect on the shape of this curve except to change porosity, and thus the upper limit of soil moisture content.

[48] With this strong dependence on soil moisture, what would happen to  $S$  if soil moisture varied with depth and time? A water table, simulated by assuming saturated soils below a specified depth, weakly amplifies  $S$ . For very shallow water tables overlapping the frozen layer,  $S$  jumps to values expected for nearly saturated conditions (not shown). Without including a full hydrological cycle in the model, we could not simulate temporal variations in soil moisture content. However, if winter soil moisture stays above 75% of saturation, the effect of seasonal variability would probably be small. In drier soils, inter-annual and decadal variability in soil moisture could produce large variability in the strength of reemergence. This indicates reemergence would respond to long-term droughts and might explain why the relationship between winter conditions and

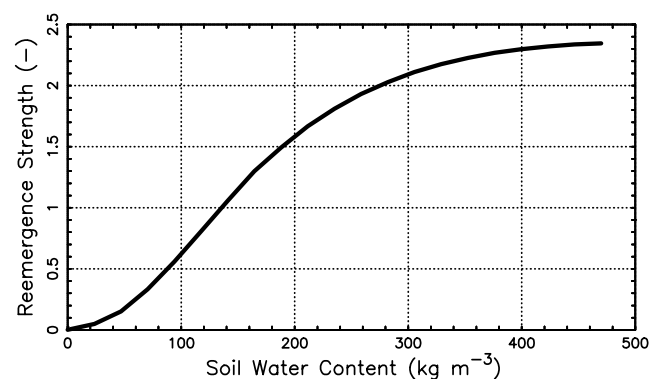


**Figure 13.** Reemergence strength for a July ground flux perturbation as a function of soil water content.

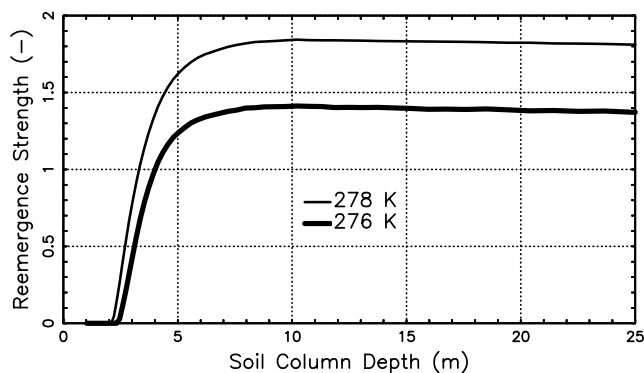


**Figure 14.** Reemergence strength for a July ground flux perturbation as a function of total soil column depth assuming annual average temperatures of 278 K and 276 K.

summer monsoon appears to strengthen and weaken over time [Lo and Clark, 2002; Robock et al., 2003].

[49] Low soil moisture may partly explain why the temperature records at some stations did not show statistically significant reemergence even though temperatures clearly dipped below freezing. Low soil moisture implies the strength of the reemergence may be less than the natural background noise, making statistical detection difficult or impossible. However, we did not have soil moisture measurements at the stations to confirm this hypothesis.

#### 5.4. Required Model Configuration

[50] To capture reemergence, our model required a soil column at least 7 m deep to ensure the total heat capacity of the entire soil column was large enough to properly represent the freezing layer. Figure 14 shows  $S$  as a function of total soil depth for  $T_{ann}$  of 278 K and 276 K and a July  $G$  perturbation. Total depths less than 2–3 m violated the conditions required to assume zero flux out of the bottom of the soil column. As a result, the entire soil column froze each year, even after the  $G$  perturbation. These results are consistent with previous studies: Lynch-Stieglitz [1994] also found unreasonably deep freezing in a model with a shallow soil depth. By comparison, the observations indicate maximum freeze depths between 1.0 and 1.5 m. With the entire soil column freezing each year, the ground ice perturbation and thus  $S$  are both zero.

[51] Beyond a critical soil depth between 2–3 m, the violation of the zero bottom flux assumption is not as severe and the heat capacity of the soil column is large enough to stabilize the frozen layer dynamics. This produces much more realistic maximum freeze depths and a sharp increase in  $S$ . The 276 K simulation has a deeper expected maximum freeze depth than the 278 K simulation, and thus a slightly deeper critical total soil depth.

[52] For total soil depths greater than  $\sim 7$  m,  $S$  abruptly levels off to a nearly constant value. The depth where this change occurs corresponds roughly to three times the damping depth,  $D$ . Only a small fraction of the anomalous heat diffuses to the deeper soil layers below  $3D$  for interannual variations in soil temperature, so further increases in soil depth have minimal effect on  $S$ . However,

the increased thermal inertia associated with deeper soil columns acts to stabilize the vertical soil temperature profile such that  $S$  approaches a constant value. Our results are consistent with previous studies indicating the soil depth required to capture variability increases with the characteristic timescale [Smerdon and Stieglitz, 2006] and a model requires a soil depth of at least  $3D$  to capture seasonal temperature variability [Sun and Zhang, 2004].

[53] As long as our model had sufficient depth, reemergence always occurred, independent of the number of soil layers. Figure 15 shows  $S$  as a function of number of soil layers assuming a total soil column depth of 4 m for a  $T_{ann}$  of 278 K and a July  $G$  perturbation. Reemergence occurred with as few as three soil layers (the minimum possible for this model), as long as the top layer froze and the bottom layer did not. The large variation in  $S$  with fewer layers results from the inability of our model to properly simulate the maximum freeze depth with such coarse vertical resolution. The simulated freeze depth converges as the number of layers increases, and the  $S$  approaches a constant value. In our model, this convergence occurs between 15–25 layers, or vertical resolutions between 0.27 and 0.16 m, which is similar in magnitude to the change in freeze depth resulting from the  $G$  perturbation. Thus to best reproduce reemergence, the vertical resolution must be high enough to capture variability in the frozen layer.

[54] Our model experiments with total soil depth and the number of soil layers indicate that not all land surface parameterizations can capture the reemergence of past soil temperature anomalies. Land surface parameterizations used in atmospheric circulation models to estimate surface fluxes of sensible and latent heat typically have total soil depths of 1–5 m with 5–20 layers. These parameterizations typically include complex interactions between surface air temperature, precipitation, vegetation, and snow depth, but the total soil depths border on the minimum capabilities required to capture reemergence. Since the freeze depth varies with location and from year-to-year, such parameterizations might only capture reemergence in some places or years, but not others. Estimates of sensible and latent heat fluxes, with possible influences on large-scale circulation, may not fully reflect the effects of soil temperature reemergence. To accurately reproduce reemergence, a model must have a soil

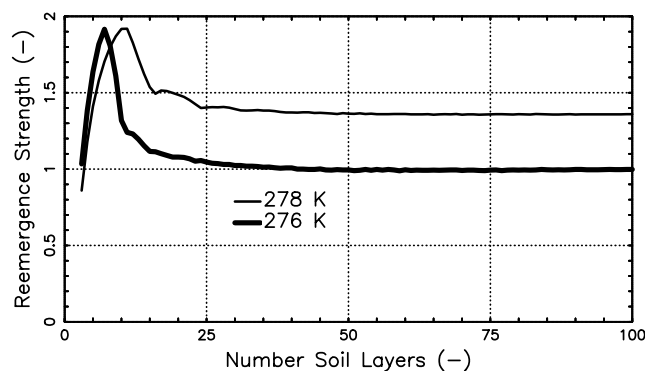


**Figure 15.** Reemergence strength for a July ground flux perturbation as a function of number of soil layers with a 4 m total soil column depth assuming annual average temperatures of 278 K and 276 K.

column at least 7 m deep with enough vertical resolution to accurately capture variability in the frozen layer.

## 6. Summary and Discussion

[55] We identified reemergence of past soil temperature anomalies in long-term records at sites across the former Soviet Union and successfully simulated reemergence using a simple soil heat transfer model with phase change. Variations in surface conditions are stored, isolated from diffusion processes, as variations in the amount of ground ice. In simplest terms, warmer soils in fall result in a shallower maximum freeze depth in winter, which requires less energy to thaw in spring, resulting in warmer soils the following summer.

[56] Reemergence strength depends on the size of the ground ice perturbation and the magnitude of the residual temperature anomaly below the maximum freeze depth. The ground ice perturbation determines how much energy is stored as latent heat. The residual temperature anomaly modulates the rapid temperature rise after soil thaw resulting from the sudden drop in  $c_a$  associated with the latent heat of fusion. Reemergence is strongest at an optimal  $T_{ann}$  representing an optimal balance between ground ice perturbation and residual temperature anomaly. Reemergence does not occur without soil water and never occurs if the soil does not freeze. To simulate reemergence requires a soil model at least 7 m deep with enough vertical resolution to capture temporal variability in the frozen layer.

[57] The presence of seasonal snow cover complicates soil temperature reemergence. Because of its thermal insulating effect, seasonal snow cover can either enhance or reduce soil freeze-thaw processes, depending on the timing, thickness, and physical and thermal properties of snow cover [Zhang, 2005]. Therefore snow cover has the potential to either amplify or dampen soil temperature reemergence. These issues are out of the scope of this article and will not be discussed. Further data analysis and numerical simulation are needed to further improve our understanding of the interactions between snow cover and reemergence.

[58] Reemergence represents a heat storage phenomenon that might help explain observed relationships between winter conditions and the summer monsoon in Asia [Robock et al., 2003] and North America [Lo and Clark, 2002]. Energy associated with near surface temperature anomalies is stored in the form of variations in the amount of ground ice. When stored as latent heat, the anomalous energy cannot influence surface fluxes of sensible and latent heat, so the effects of land memory disappear in winter. When the soil thaws, the latent energy is put back into the soil and reappears as a temperature anomaly at the surface.

[59] The reemergence of past soil temperature anomalies and associated influence on surface energy fluxes represents a new class of time delayed, land-ocean-atmosphere feedbacks. The underlying mechanism is the storage of energy in the form of variations in the amount of latent heat, so temperature reemergence could occur anywhere we see seasonal and interannual variations in the amount of frozen water, such as soils, sea ice, lake ice, and glaciers. Temperature reemergence has a broad variety of potentially useful applications. For example, knowledge of winter soil temperature and freeze depth can be used to predict summer

soil temperature, possibly improving short-term or seasonal climate prediction (6–12 months) in regions with seasonally frozen soil.

[60] **Acknowledgments.** We would like to express our gratitude to the three anonymous reviewers for their insightful and constructive suggestions and comments. This research was funded by the National Research Council Research Associateship Program to the Earth System Research laboratory, National Oceanic and Atmospheric Administration, Boulder; the U.S. National Aeronautics and Space Administration (NASA) grant NNX06AE65G, the U.S. National Science Foundation (NSF) grants OPP-0229766 and OPP-0352910 to the National Snow and Ice Data center, University of Colorado; and the NSF cooperative agreement OPP-0327664 through the International Arctic Research Center and the U.S. NASA grants NNG05GD15G, NNX06AE65G, and NNG06CG42G, and NASA Subcontract NNG05GF41G to the Department of Atmospheric Science, Colorado State University. Any opinions, findings, and conclusions are those of the authors and do not necessarily represent the views of the above funding agencies.

## References

- Alexander, M., and C. Deser (1995), A mechanism for the recurrence of wintertime Midlatitude SST anomalies, *J. Phys. Oceanogr.*, *25*, 122–137.
- Amenu, G. G., P. Kumar, and X. Z. Liang (2005), Interannual variability of deep-layer hydrologic memory and mechanisms of its influence on surface energy fluxes, *J. Clim.*, *18*, 5024–5045.
- Bartlett, M. G., D. S. Chapman, and R. N. Harris (2005), Snow effect on North American ground temperatures, 1950–2002, *J. Geophys. Res.*, *110*, F03008, doi:10.1029/2005JF000293.
- Bhatta, U. S., E. K. Schneiderb, and D. G. Dewitt (2003), Influence of North American land processes on North Atlantic Ocean variability, *Global Planet. Change*, *37*, 33–56.
- Bonan, G. B. (1996), A Land Surface Model (LSM Version 1.0) for Ecological, Hydrological, and Atmospheric Studies: Technical Description and Users Guide, *NCAR Technical Note NCAR/TN-417+STR*, Boulder Colorado.
- Carslaw, H. S., and J. C. Jaeger (1959), *Conduction of Heat in Solids*, 2nd ed., 510 pp., Oxford Univ. Press, New York.
- Deser, C., M. A. Alexander, and M. S. Timlin (2003), Understanding the persistence of sea surface temperature anomalies in midlatitudes, *J. Clim.*, *16*, 57–72.
- Elias, E. A., R. Cichota, H. H. Torriani, and Q. J. van Lier (2004), Analytical soil-temperature model: Correction for temporal variation of daily amplitude, *Soil Sci. Soc. Am. J.*, *68*, 784–788.
- Fuchs, M., G. S. Campbell, and R. I. Papendick (1978), An analysis of sensible and latent heat flow in partially frozen unsaturated soil, *Soil Sci. Soc. Am. J.*, *42*(3), 379–385.
- Gao, R., Z. G. Wei, W. J. Dong, and H. L. Zhong (2005), Impact of the anomalous thawing in the Tibetan Plateau on summer precipitation in China and its mechanism, *Adv. Atmos. Sci.*, *22*(2), 238–245.
- Gilichinsky, D. A., R. G. Barry, S. S. Bykhovets, V. A. Sorokovikov, T. Zhang, S. L. Zudin, and D. G. Fedorov-Davydov (1998), A century of temperature observations of soil climate: methods of analysis and long-term trends, *Proceedings of the 7th International Conference on Permafrost*, Yellowknife, Canada, June 22–27, 313–317.
- Hillel, D. (1998), *Environmental Soil Physics*, Academic Press, 771 pp.
- Hu, Q., and S. Feng (2003), A daily soil temperature dataset and soil temperature climatology of the contiguous United States, *J. Appl. Meteorol.*, *42*, 1139–1156.
- Hu, Q., and S. Feng (2004), A role of the soil enthalpy in land memory, *J. Clim.*, *17*(18), 3633–3643.
- Kane, D. L., K. M. Hinkel, D. J. Goering, L. D. Hinzman, and S. I. Outcalt (2001), Non-conductive heat transfer associated with frozen soils, *Global Planet. Change*, *29*, 275–292.
- Liebenthal, C., and T. Foken (2007), Evaluation of six parameterization approaches for the ground heat flux, *Theor. Appl. Climatol.*, *88*(1–2), 43–56.
- Ling, F., and T. Zhang (2004), A numerical model for surface energy balance and thermal regime of the active layer and permafrost containing unfrozen water, *Cold Regions Sci. Tech.*, *38*, 1–15.
- Ling, F., and T. Zhang (2005), Modeling the effect of variations in snow-pack-disappearance date on surface-energy balance on the Alaskan North Slope, *Arctic, Antarctic, Alpine Res.*, *37*(4), 483–489.
- Lo, F., and M. Clark (2002), Relationships between Spring Snow Mass and Summer Precipitation in the Southwestern United States Associated with the North American Monsoon System, *J. Clim.*, *15*, 1378–1385.
- Lukianov, V. S., and M. D. Golovko (1957), Calculation of the depth of freeze in soils, *Bull 23 Union of Transp. Constr.*, Moscow.

- Lynch-Stieglitz, M. (1994), The development and validation of a simple snow model for the GISS GCM, *J. Clim.*, *7*, 1842–1855.
- Osterkamp, T. E. (2005), The recent warming of permafrost in Alaska, *Global Planet. Change*, *49*(3–4), 187–202.
- Pan, H. L., and L. Mahrt (1987), Interaction between soil hydrology and boundary-layer development, *Bound. Layer Meteorol.*, *38*(1–2), 185–202.
- Peters-Lidard, C. D., E. Blackburn, X. Liang, and E. F. Wood (1998), The effect of soil thermal conductivity parameterization on surface energy fluxes and temperatures, *J. Atmos. Sci.*, *55*, 1209–1224.
- Robock, A., M. Q. Mu, K. Vinnikov, and D. Robinson (2003), Land surface conditions over Eurasia and Indian summer monsoon rain, *J. Geophys. Res.*, *108*(D4), 4131, doi:10.1029/2002JD002286.
- Schaefer, K., A. S. Denning, and O. Leonard (2005), The winter Arctic Oscillation, the timing of spring, and carbon fluxes in the Northern Hemisphere, *Global Biogeochem. Cycles*, *19*(3), GB3017, doi:10.1029/2004GB002336.
- Smerdon, J. E., and M. Stieglitz (2006), Simulating heat transport of harmonic temperature signals in the Earth's shallow subsurface: Lower-boundary sensitivities, *Geophys. Res. Lett.*, *33*, L14402, doi:10.1029/2006GL026816.
- Smerdon, J. E., H. N. Pollack, J. W. Enz, and M. J. Lewis (2003), Conduction-dominated heat transport of the annual temperature signal in soil, *J. Geophys. Res.*, *108*(B9), 2431, doi:10.1029/2002JB002351.
- Sun, S., and X. Zhang (2004), Effect of the lower boundary position of the Fourier equation on the soil energy balance, *Adv. Atmos. Sci.*, *21*, 868–878.
- Tang, M., and E. R. Reiter (1986), The similarity between the maps of soil temperature in U.S. and precipitation anomaly of the subsequent season, *Plateau Meteorol.*, *5*, 293–307.
- Wang, G. L., and L. Z. You (2004), Delayed impact of the North Atlantic Oscillation on biosphere productivity in Asia, *Geophys. Res. Lett.*, *31*(12), L12210, doi:10.1029/2004GL019766.
- Zhang, T. (2005), Influence of the seasonal snow cover on the ground thermal regime: An overview, *Rev. Geophys.*, *43*, RG4002, doi:10.1029/2004RG000157.
- Zhang, T., R. Barry, and D. Gilichinsky, compilers (2001a), *Russian historical soil temperature data*, National Snow and Ice Data Center, digital media, Boulder, CO.
- Zhang, T., R. G. Barry, D. Gilichinsky, S. S. Bykhovets, V. A. Sorokovikov, and J. P. Ye (2001b), An amplified signal of climatic change in soil temperatures during the last century at Irkutsk, *Russian Clim. Change*, *49*, 41–76.

---

K. M. Schaefer and T. Zhang, National Snow and Ice Data Center, Cooperative Institute for Research in Environmental Sciences, University of Colorado at Boulder, Boulder, CO, USA. (kevin.schaefer@nsidc.org)

R. Stöckli, Department of Atmospheric Science, Colorado State University, Boulder, CO, USA.

P. P. Tans, Earth System Research Laboratory, National Oceanic and Atmospheric Administration, Boulder, CO, USA.